New Processes in the Environmental Chemistry of Nitrite. 2. The Role of Hydrogen Peroxide

ARTICLE *in* ENVIRONMENTAL SCIENCE AND TECHNOLOGY · OCTOBER 2003

Impact Factor: 5.33 · DOI: 10.1021/es0300259 · Source: PubMed

6 AUTHORS, INCLUDING:

Davide Vione
Università degli Studi di Torino
265 PUBLICATIONS **3,749** CITATIONS
SEE PROFILE

Valter Maurino
Università degli Studi di Torino
203 PUBLICATIONS **4,005** CITATIONS
SEE PROFILE

Claudio Minero
Università degli Studi di Torino
329 PUBLICATIONS **8,126** CITATIONS
SEE PROFILE

Environ. Sci. Technol. **2003**, *37,* 4635−4641

New Processes in the Environmental Chemistry of Nitrite. 2. The Role of Hydrogen Peroxide

DAVIDE VIONE, VALTER MAURINO, CLAUDIO MINERO, DANIELE BORGHESI, MIRCO LUCCHIARI, AND EZIO PELIZZETTI*

Dipartimento di Chimica Analitica, Università di Torino, Via P. Giuria 5, 10125 Torino, Italy

The oxidation of nitrite and nitrous acid to $^{\bullet}NO_2$ upon irradiation of dissolved Fe(III), ferric (hydr)oxides, and nitrate has previously been shown to enhance phenol nitration. This allowed the proposal of a new role for nitrite and nitrous acid in natural waters and atmospheric aerosols. This paper deals with the interaction between hydrogen peroxide, a key environmental factor in atmospheric oxidative chemistry, and nitrite/nitrous acid. The reaction between nitrous acid and hydrogen peroxide yields peroxynitrous acid, a powerful nitrating agent and an important intermediate in atmospheric chemistry. The kinetics of this reaction is compatible with a rate-determining step involving either $H_3O_2^+$ and HNO_2 or H_2O_2 and protonated nitrous acid. In the former case the rate constant between the two species would be $179.6 \pm 1.4\ M^{-1}\ s^{-1}$, in the latter case it would be as high as $(1.68 \pm 0.01) \times 10^{10}\ M^{-1}\ s^{-1}$ (diffusion-controlled reaction). Due to the more reasonable value of the rate constant, the reaction between $H_3O_2^+$ and HNO_2 seems more likely. In the presence of $HNO_2 + H_2O_2$ the nitration of phenol is strongly enhanced when compared with HNO_2 alone. The nitration rate of phenol in the presence of peroxynitrous acid decreases as pH increases, thus HOONO is a potential source of atmospheric nitroaromatic compounds in acidic water droplets. The mixture Fe(II) + H_2O_2 (Fenton reagent) can oxidize nitrite and nitrous acid to nitrogen dioxide, which results in phenol nitration. The nitration in the presence of Fe(II) + H_2O_2 + NO_2^-/HNO_2 occurs more rapidly than the one with H_2O_2 + NO_2^-/HNO_2 at pH 5, where little HNO_2 is available to directly react with hydrogen peroxide. Both systems, however, are more effective than NO_2^-/HNO_2 alone in producing nitrophenols from phenol. Another process leading to the oxidation of nitrite to nitrogen dioxide is the photo-Fenton one. It can be relevant at pH ≥ 6, as nitrite does not react with H_2O_2 at room temperature. Under such conditions the source of Fe(II) is the photolysis of ferric (hydr)-oxides (heterogeneous photo-Fenton reaction). In the presence of nitrite this reaction induces very effective nitrophenol formation from phenol.

Introduction

The reactions involving aromatic compounds in the atmosphere are a matter of concern, due to the effects of the transformation intermediates on human health and the environment. Nitration processes play a relevant role in this context, as they yield for instance mutagenic nitro-PAHs (*1*−*3*) and phytotoxic nitrophenols (*4*−*6*). Gas-phase nitration processes have been extensively studied. They are very similar for both PAHs and phenols and include $^{\bullet}OH$- and $^{\bullet}NO_3$-mediated nitration (*1*, *2*, *4*, *5*, *7*, *8*). Much interest has recently been focused on the condensed-phase nitration of aromatic compounds (pyrene (*9*, *10*), phenols (*11*−*15*), azaarenes (*16*)), adsorbed on oxides or in solution, in the presence of nitrogen dioxide, nitrate, and nitrite, in the dark and under irradiation.

The photolysis of nitrite and nitrous acid is a relevant source of $^{\bullet}OH$ in the environment (*17*), but it also yields nitrogen dioxide (*18*):

$$NO_2^- + h\nu + H^+ \rightarrow {}^{\bullet}NO + {}^{\bullet}OH \quad [\Phi_{1,\,360\ nm} = 0.025] \quad (1)$$

$$NO_2^- + {}^{\bullet}OH \rightarrow {}^{\bullet}NO_2 + OH^- \quad [k_2 = 1.0 \times 10^{10}\ M^{-1}\ s^{-1}] \quad (2)$$

$$HNO_2 + h\nu \rightarrow {}^{\bullet}NO + {}^{\bullet}OH \quad [\Phi_{3,\,360\ nm} = 0.32] \quad (3)$$

$$HNO_2 + {}^{\bullet}OH \rightarrow {}^{\bullet}NO_2 + H_2O \quad [k_4 = 2.6 \times 10^{9}\ M^{-1}\ s^{-1}] \quad (4)$$

Nitrophenols form in the presence of phenol and nitrite under irradiation, most likely due to the photoinduced formation of $^{\bullet}NO_2$ (*19*). We have recently shown that the photoinduced oxidation of nitrite and nitrous acid to $^{\bullet}NO_2$ upon irradiation of dissolved Fe(III), ferric (hydr)oxides, and nitrate yields nitrophenols at a higher extent than the irradiation of nitrite and nitrous acid alone. This is particularly true when the concentration of nitrite or nitrous acid is very low (*20*). For instance, the thermal nitration of phenol by HNO_2 prevails upon the nitration via HNO_2 photolysis (*21*), but in the presence of Fe(III) and HNO_2 the photoinduced nitration process prevails over the thermal one (*20*). The photolysis of $[Fe(OH)(H_2O)_5]^{2+}$ yields $^{\bullet}OH$ (*22*), which can then oxidize nitrous acid (reactions 5 and 4):

$$[Fe(OH)(H_2O)_5]^{2+} + h\nu + H_2O \rightarrow [Fe(H_2O)_6]^{2+} + {}^{\bullet}OH \quad [\Phi_{5,\,310\ nm} = 0.19] \quad (5)$$

This is one of the first examples of interaction between different environmental factors.

The present paper reports the results of studies carried out on the interaction between nitrite or nitrous acid at mM concentration and hydrogen peroxide, a widespread atmospheric oxidant (*23*, *24*). It is necessary to differentiate between the reactivity of hydrogen peroxide alone and that arising from the activation by Fe(II) (Fenton reaction (*25*)).

Phenol was chosen in this work as a model aromatic molecule. The formation of nitrophenols from phenol can take place via two pathways: one is the direct nitration of phenol to nitrophenols, the other involves first phenol nitrosation to yield 4-nitrosophenol (and possibly 2-nitrosophenol), followed by the oxidation of the nitrosoderivatives to the nitroderivatives (*15*, *19*). An assessment of the relative weight of the two pathways (*20*) was carried out in the systems under study in the present work, and the results indicate that the first pathway strongly prevails over the second one.

Experimental Section

Reagents and Materials. Phenol (P), 2-nitrophenol (2NP), 4-nitrophenol (4NP), and 4-nitrosophenol (4NOP) (purity grade >98%) were purchased from Aldrich, $NaNO_2$ (>97%)

* Corresponding author phone: +39-011-6707630; fax: +39-011-6707615; e-mail: ezio.pelizzetti@unito.it.

10.1021/es0300259 CCC: $25.00
Published on Web 09/10/2003

and $FeSO_4 \cdot 7H_2O$ (99.5%) from Carlo Erba, $HClO_4$ (70%) and H_2O_2 (35%) from Merck. All reagents were used as received without further purification. Acetonitrile and 2-propanol were LiChrosolv gradient grade, purchased from Merck. α-Fe_2O_3 and β-FeOOH have been synthesized following the procedures given by Leland and Bard (*26*).

Irradiation Experiments. Irradiation was carried out in cylindrical, magnetically stirred Pyrex glass cells (4.0 cm diameter, 2.3 cm height), containing 5 mL of aqueous solution (or suspension).

As a radiation source we used a set of 3 × 40 W Philips TL K05 lamps with emission maximum at 360 nm. The total photon flux in the cells was 3.8×10^{-7} Ein s^{-1}, actinometrically determined using the ferrioxalate method (*27*). The emission spectrum of the lamp, together with the absorption spectra of nitrite and nitrous acid, are reported elsewhere (*20*). After irradiation the solutions were directly analyzed, while the suspensions were first filtered through 0.45 μm filter membranes (cellulose acetate, Millipore). Dark experiments were carried out in magnetically stirred vials, and sample pretreatment and analysis executed in the same way as for irradiation experiments.

Analytical Determinations. The HPLC determinations were carried out with a Merck-Hitachi HPLC, using a RP-C18 LichroCART column (Merck, length 125 mm, diameter 4 mm) packed with LiChrospher 100 RP-18 (5 μm diameter). P, 2NP, 4NP, and 4NOP were isocratically eluted with a 30/70 mixture of acetonitrile/ $H_3PO_4 + NaH_2PO_4$ (2×10^{-2} M total phosphate, pH 2.8) and detected at 210 nm, with the exception of 4NOP that was detected at 315 nm. Under these conditions the retention times were (min) as follows: P (3.75), 2NP (9.30), 4NP (5.10), 4NOP (2.05). The retention time corresponding to the void volume was 0.90 min.

Spectrophotometric determinations were carried out with a Varian Cary "100 Scan" UV−vis spectrophotometer. pH measures were executed with a Metrohm 713 pH-meter. Water used was Milli-Q quality.

Stopped-Flow Experiments. Some stopped-flow measures were carried out to study the kinetics of the reaction between HNO_2 and H_2O_2, using a High-Tech stopped-flow spectrophotometer, equipped with a temperature control device (set at 25°C) and connected with an Agilent Infiniium oscilloscope (500 MHz, 1 GSa/s) for data acquisition. The disappearance of HNO_2 was monitored measuring the absorbance at 332 nm, where $\epsilon_{HNO2} = \epsilon_{NO2-}$. At this wavelength there is no spectral interference by other species in the system.

Determination of the Initial Rates. The disappearance of nitrous acid upon reaction with hydrogen peroxide as determined in the stopped-flow measures was approximated with a pseudo-first-order kinetics. Assume C_{H2O2} as the total concentration of hydrogen peroxide and $C_{NaNO2} = [HNO_2] + [NO_2^-]$. If $C_{H2O2} \geq C_{NaNO2}$, the time evolution of nitrous acid + nitrite absorbance can be approximated by $A_t = A_0 \times \exp(-k_d \times t)$. A_0 is the initial absorbance of nitrite + nitrous acid, A_t the absorbance at time t, and k_d the pseudo-first-order rate constant (s^{-1}). The initial disappearance rate of nitrous acid is given by $\alpha_{HNO2} \times C_{NaNO2} \times k_d$, where $\alpha_{HNO2} \times C_{NaNO2}$ is the initial concentration of nitrous acid. If $C_{H2O2} < C_{NaNO2}$, the absorbance will decrease until it reaches a constant, nonzero value (A_∞). In such a case the time evolution of the absorbance can be approximated by $A_t = (A_0 - A_\infty) \times \exp(-k_d \times t) + A_\infty$, and the initial disappearance rate of HNO_2 is $[(A_0 - A_\infty)/A_0] \times a_{HNO2} \times C_{NaNO2} \times k_d$. The reaction rate has been determined at 25 °C for different reaction conditions, together with the associated standard deviation ($\pm 1\sigma$, see Table 1).

The disappearance of phenol and the formation of nitrophenols were followed at different times. The time evolution of phenol concentration [P] follows with good approximation a pseudo-first-order kinetics. In the general case it is $[P] = ([P]_0 - [P]_\infty) \times \exp(-k^d_P \times t) + [P]_\infty$, where k^d_P is the pseudo-first-order rate constant for phenol degradation, determined by fitting the [P] vs time data, $[P]_0$ is the initial phenol concentration, and $[P]_\infty$ is the residual phenol at $t \rightarrow \infty$ (if phenol degradation will not be complete due to defect of the reactant, otherwise $[P]_\infty = 0$). The initial rate of phenol degradation is $k^d_P([P]_0 - [P]_\infty)$. The time evolution of either 2NP or 4NP is described by $[NP] = k^f_{NP}([P]_0 - [P]_\infty) \times (k^d_{NP} - k^d_P)^{-1} \times [\exp(-k^d_P \times t) - \exp(-k^d_{NP} \times t)]$, the corresponding initial formation rate being $k^f_{NP}([P]_0 - [P]_\infty)$. In many a case $[P]_\infty = 0$. For further details see ref *20*. The initial rates for phenol and nitrophenols are reported in Tables 2 and 3, together with the associated standard deviation ($\pm 1\sigma$).

TABLE 1. Initial Disappearance Rate of HNO_2 in the Presence of H_2O_2[a]

no.	C_{H2O2}, M	C_{NaNO2}, M	pH	α_{HNO2}	HNO_2 degr rate, M s^{-1}
1		0.005	2.0	0.94	$(2.00 \pm 0.01) \times 10^{-6}$
2	0.003	0.005	2.0	0.94	$(6.06 \pm 0.04) \times 10^{-4}$
3	0.005	0.005	2.0	0.94	$(1.02 \pm 0.03) \times 10^{-3}$
4	0.010	0.005	2.0	0.94	$(1.86 \pm 0.02) \times 10^{-3}$
5	0.015	0.005	2.0	0.94	$(2.91 \pm 0.03) \times 10^{-3}$
6	0.020	0.005	2.0	0.94	$(3.92 \pm 0.02) \times 10^{-3}$
7	0.005	0.002	2.0	0.94	$(4.21 \pm 0.05) \times 10^{-4}$
8	0.005	0.003	2.0	0.94	$(5.87 \pm 0.02) \times 10^{-4}$
9	0.005	0.004	2.0	0.94	$(7.97 \pm 0.03) \times 10^{-4}$
10	0.005	0.006	2.0	0.94	$(1.15 \pm 0.01) \times 10^{-3}$
11	0.005	0.008	2.0	0.94	$(1.49 \pm 0.01) \times 10^{-3}$
12	0.005	0.010	2.0	0.94	$(1.88 \pm 0.01) \times 10^{-3}$
13	0.005	0.015	2.0	0.94	$(2.86 \pm 0.02) \times 10^{-3}$
14	0.005	0.020	2.0	0.94	$(3.91 \pm 0.02) \times 10^{-3}$
15	0.010	0.005	0.5	1.00	$(6.92 \pm 0.06) \times 10^{-3}$
16	0.010	0.005	1.0	0.99	$(5.64 \pm 0.04) \times 10^{-3}$
17	0.010	0.005	1.5	0.98	$(3.53 \pm 0.03) \times 10^{-3}$
18	0.010	0.005	2.0	0.94	$(1.80 \pm 0.01) \times 10^{-3}$
19	0.010	0.005	2.5	0.83	$(6.52 \pm 0.06) \times 10^{-4}$
20	0.010	0.005	3.0	0.61	$(1.31 \pm 0.01) \times 10^{-4}$
21	0.010	0.005	3.5	0.33	$(1.12 \pm 0.01) \times 10^{-5}$
22	0.010	0.005	4.0	0.14	$(2.83 \pm 0.02) \times 10^{-6}$

[a] Reaction temperature 25 °C. Other conditions are reported in the table. Error = standard deviation (σ), obtained from the goodness of the fit to the experimental data, representing intraseries variability. Entries #4 and #18 represent results of duplicate runs.

The uncertainty on the initial rates has been obtained from the goodness of the fit between the theoretical curves and the experimental data. As a consequence the error bounds of the data reported in Tables 1−3 represent an intraseries variability, since all the experiments relative to the same curve have been carried out as close as possible in time. The error on the initial rates as measured in the stopped-flow runs (see Table 1) is much lower than the one associated with HPLC measures (Tables 2 and 3). This happens because in the former case the fitting was carried out on 20−30 experimental points, while in the case of the HPLC only 4 to 6 data points are usually available. As to the interseries variability (difference between the rates measured at some days' distance), it ranges from about 4% for the stopped-flow runs (thermostatic system) up to 10% for HPLC measures, as could be inferred from the results of some runs made in duplicate (see Table 1, entries #4 and #18, and Table 2, entries #4 and #17).

Results and Discussion

We studied the transformation of phenol in different systems (HNO_2, H_2O_2/HNO_2, Fe(II)/H_2O_2/HNO_2+NO_2^-, α-Fe_2O_3/NO_2^-/H_2O_2/UV, β-FeOOH/NO_2^-/H_2O_2/UV), with a particular focus on the formation of nitrophenols as intermediates. The yield of transformed phenol into nitrophenols (2NP, 4NP) is usually in the range 10−70% depending on the particular system under consideration (compare the initial rates reported in Tables 2 and 3). Among the other transformation

TABLE 2. Initial Degradation Rate of P, Initial Formation Rates of 2NP and 4NP, in the Dark[a]

no.	conditions	pH	P degr rate, M s^{-1}	2NP form. rate, M s^{-1}	4NP form. rate, M s^{-1}
1	P, HNO_2, H_2O_2	1.5	$(5.65 \pm 0.03) \times 10^{-6}$	$(1.91 \pm 0.04) \times 10^{-6}$	$(1.43 \pm 0.03) \times 10^{-6}$
2	P, HNO_2, H_2O_2	2.0	$(1.17 \pm 0.01) \times 10^{-6}$	$(3.92 \pm 0.20) \times 10^{-7}$	$(2.76 \pm 0.17) \times 10^{-7}$
3	P, HNO_2, H_2O_2	2.5	$(6.88 \pm 0.08) \times 10^{-7}$	$(1.55 \pm 0.06) \times 10^{-7}$	$(1.09 \pm 0.01) \times 10^{-7}$
4	P, HNO_2, H_2O_2	3.0	$(2.22 \pm 0.04) \times 10^{-7}$	$(2.84 \pm 0.09) \times 10^{-8}$	$(2.22 \pm 0.03) \times 10^{-8}$
5	P, HNO_2, H_2O_2	3.5	$(4.40 \pm 0.01) \times 10^{-8}$	$(8.97 \pm 0.36) \times 10^{-9}$	$(3.54 \pm 0.03) \times 10^{-9}$
6	P, HNO_2, H_2O_2	4.0	$(4.78 \pm 0.04) \times 10^{-9}$	$(7.94 \pm 0.83) \times 10^{-10}$	$(5.22 \pm 0.54) \times 10^{-10}$
7	P, HNO_2, H_2O_2, 0.10 M 2-propanol	1.5	$(6.46 \pm 0.06) \times 10^{-8}$	$(3.31 \pm 0.06) \times 10^{-8}$	$(2.69 \pm 0.13) \times 10^{-8}$
8	P, HNO_2, H_2O_2, 0.10 M 2-propanol	2.0	$(8.68 \pm 0.12) \times 10^{-8}$	$(3.93 \pm 0.18) \times 10^{-8}$	$(2.92 \pm 0.23) \times 10^{-8}$
9	P, HNO_2, H_2O_2, 0.10 M 2-propanol 0.10 M	2.5	$(8.95 \pm 0.18) \times 10^{-8}$	$(1.90 \pm 0.05) \times 10^{-8}$	$(1.50 \pm 0.07) \times 10^{-8}$
10	P, HNO_2, H_2O_2, 0.10 M 2-propanol 0.10 M	3.0	$(1.29 \pm 0.03) \times 10^{-7}$	$(8.91 \pm 0.14) \times 10^{-9}$	$(5.72 \pm 0.14) \times 10^{-9}$
11	P, HNO_2, H_2O_2, 0.10 M 2-propanol	3.5	$(6.00 \pm 0.07) \times 10^{-8}$	$(5.15 \pm 0.32) \times 10^{-9}$	$(3.04 \pm 0.26) \times 10^{-9}$
12	P, HNO_2, H_2O_2, 0.10 M 2-propanol	4.0	$(1.28 \pm 0.01) \times 10^{-9}$	$(5.23 \pm 0.42) \times 10^{-10}$	$(3.67 \pm 0.20) \times 10^{-10}$
13	P, HNO_2	4.0	$(1.56 \pm 0.01) \times 10^{-9}$	$(8.75 \pm 1.22) \times 10^{-11}$	$(8.60 \pm 1.69) \times 10^{-11}$
14	P, Fe(II), HNO_2, H_2O_2	5.0	$(1.74 \pm 0.32) \times 10^{-6}$	$(2.23 \pm 0.56) \times 10^{-8}$	$(1.81 \pm 0.49) \times 10^{-8}$
15	P, HNO_2, H_2O_2	5.0	$(2.07 \pm 0.18) \times 10^{-7}$	$(2.73 \pm 0.35) \times 10^{-10}$	$(2.45 \pm 0.26) \times 10^{-10}$
16	P, HNO_2	5.0	$(8.09 \pm 1.12) \times 10^{-9}$	$(3.32 \pm 0.47) \times 10^{-11}$	$(2.23 \pm 0.39) \times 10^{-11}$
17	P, HNO_2, H_2O_2	3.0	$(2.37 \pm 0.07) \times 10^{-7}$	$(3.02 \pm 0.12) \times 10^{-8}$	$(2.26 \pm 0.02) \times 10^{-8}$

[a] Initial conditions: 2.0×10^{-4} M P, 1.0×10^{-3} M $NaNO_2$, 1.0×10^{-3} M H_2O_2 (when present), 1.0×10^{-3} M $FeSO_4$ (when present); pH adjusted with $HClO_4$. Error = standard deviation (σ), obtained from the goodness of the fit to the experimental data, representing intraseries variability. Entries #4 and #17 represent results of duplicate runs.

TABLE 3. Initial Degradation Rate of P and Initial Formation Rates of 2NP and 4NP in the Presence of Ferric (Hydr)oxides under 360 nm Irradiation[a]

no.	conditions	λ (nm)	pH	P degr. rate, M s^{-1}	2NP form. rate, M s^{-1}	4NP form. rate, M s^{-1}
1	P + $NaNO_2$	360	6.0	$(2.71 \pm 0.04) \times 10^{-8}$	$(2.96 \pm 0.46) \times 10^{-10}$	$(2.70 \pm 0.74) \times 10^{-10}$
2	P + $NaNO_2$ + α-Fe_2O_3	360	6.0	$(4.68 \pm 0.16) \times 10^{-8}$	$(1.85 \pm 0.11) \times 10^{-8}$	$(1.54 \pm 0.07) \times 10^{-8}$
3	P + $NaNO_2$ + α-Fe_2O_3+H_2O_2	360	6.0	$(1.03 \pm 0.09) \times 10^{-7}$	$(2.86 \pm 0.04) \times 10^{-8}$	$(2.17 \pm 0.03) \times 10^{-8}$
4	P + $NaNO_2$ + β-FeOOH	360	6.0	$(9.24 \pm 0.36) \times 10^{-8}$	$(7.08 \pm 0.34) \times 10^{-9}$	$(5.06 \pm 0.26) \times 10^{-9}$
5	P +$NaNO_2$ + β-FeOOH + H_2O_2	360	6.0	$(1.25 \pm 0.06) \times 10^{-7}$	$(2.38 \pm 0.16) \times 10^{-8}$	$(1.72 \pm 0.07) \times 10^{-8}$

[a] Initial conditions: 1.0×10^{-3} M P, 1.0×10^{-3} M $NaNO_2$; 0.20 g/L α-Fe_2O_3 and β-FeOOH (when present), 1.0×10^{-2} M H_2O_2 (when present). Error = standard deviation (σ), obtained from the goodness of the fit to the experimental data, representing intraseries variability.

intermediates, phenol hydroxyderivatives (catechol and hydroquinone) are present in all the systems but HNO_2 in the dark, which is not surprising since in all the other cases $^{\bullet}OH$ radicals are formed, either thermally or photochemically. The further transformation of hydroxylated phenols under the conditions we adopted can yield both the trihydroxybenzenes (which however all coelute under the HPLC conditions we used) and 1,4-benzoquinone. In the presence of nitrous acid in the dark or of nitrite under irradiation (yielding N_2O_3), also 4-nitrosophenol forms from phenol. The oxidation of 4-nitrosophenol to 4NP (*19*) has been studied and shown to contribute at a negligible level to the formation of 4NP in the systems under the present study, but it is, for instance, the main source of 4NP upon nitrite photolysis in basic solution (*15*).

The various systems will now be described in further detail as far as the formation of nitrophenols from phenol is concerned.

H_2O_2/HNO_2. Figure 1 shows the time evolution of P (initial concentration 2.0×10^{-4} M), 2NP, and 4NP in the presence of 1 mM $NaNO_2$ and of 1 mM $NaNO_2$ + 1 mM H_2O_2, at pH 3.0 ($[HNO_2] \approx 1.6 \times [NO_2^-]$ (*21*)), adjusted by addition of $HClO_4$. It can be seen that the formation of nitrophenols is much faster in the presence of $HNO_2 + H_2O_2$ than of HNO_2 alone. Phenol nitration by nitrous acid alone is likely to be an HNO_2-driven process (*28*, *29*). Phenol nitration by H_2O_2 + HNO_2 is due to the formation of peroxynitrous acid, HOONO, in the presence of hydrogen peroxide and nitrous acid (reaction 6 (*30*)). Nitrite does not react with hydrogen peroxide at an appreciable rate.

$$H_2O_2 + HNO_2 \rightarrow HOONO + H_2O \quad (6)$$

Peroxynitrous acid is an important intermediate in the interconversion of nitrogen-containing species (*31*) and a

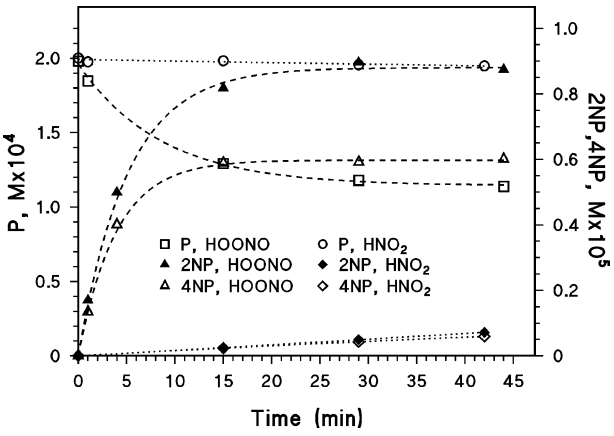

FIGURE 1. Time evolution of P, 2NP, and 4NP in the presence of 2.0×10^{-4} M P and 1.0×10^{-3} M $NaNO_2$, with and without 1.0×10^{-3} M H_2O_2, in the dark. pH 3.0 by addition of $HClO_4$.

nitrating agent (*32*). It forms in reaction 6, upon nitrate photolysis (*33*), and upon reaction between nitric oxide and superoxide (*34*). It has $pK_a = 7.0$ and is thought to play a relevant role in aqueous atmospheric chemistry (*31*).

$$NO_3^- + h\nu + H^+ \rightarrow HOONO \quad [\Phi_{7,\,254\,nm} = 0.09] \quad (7)$$

$$^{\bullet}NO + O_2^{-\bullet} + H^+ \rightarrow HOONO \quad [k_8 = 4.3 \times 10^9\ M^{-1}\ s^{-1}] \quad (8)$$

$$HOONO \rightleftarrows OONO^- + H^+ \quad [pK_{a,9} = 7.0] \quad (9)$$

Peroxynitrous acid is not stable in solution and quickly decomposes forming nitrate as the main transformation

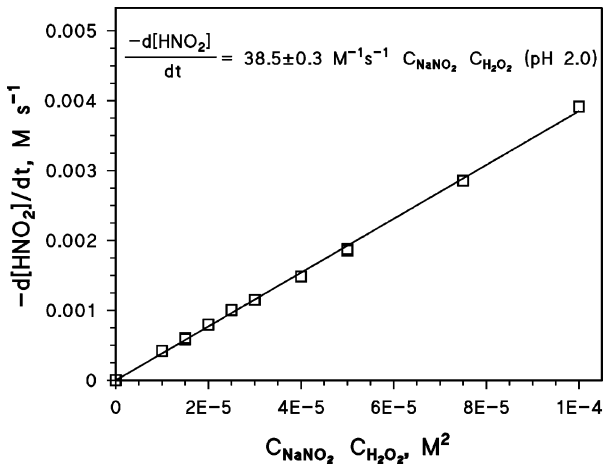

FIGURE 2. Initial transformation rates of HNO_2 as a function of $C_{NaNO2} \times C_{H2O2}$; pH 2.0 by addition of $HClO_4$. Data derived from stopped-flow spectrophotometric measures at 25 °C.

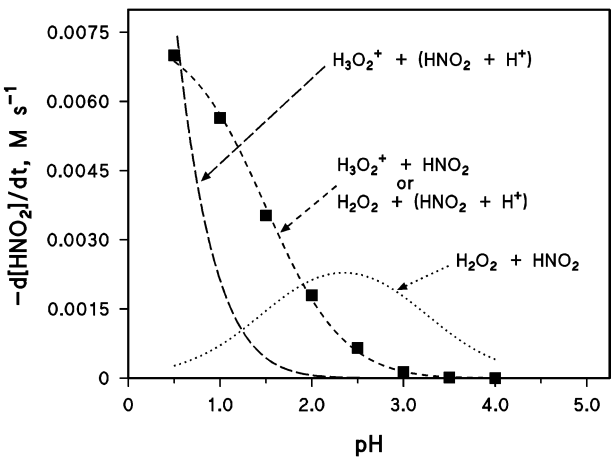

FIGURE 3. Initial transformation rates of HNO_2 ($C_{NaNO2} = 5.0 \times 10^{-3}$ M, $C_{H2O2} = 1.0 \times 10^{-2}$ M) as a function of pH, adjusted by addition of $HClO_4$. The expected pH trends of the reactions of $H_2O_2 + HNO_2$, $H_3O_2^+ + HNO_2$, H_2O_2 + protonated HNO_2, and $H_3O_2^+$ + protonated HNO_2 are shown on the Figure. Data derived from stopped-flow spectrophotometric measures at 25 °C.

product. The isomerization of HOONO to nitrate is thought to take place via reactions 11−13, which also yield free •OH and $^{\bullet}NO_2$ (*34*, *35*):

$$HOONO \rightarrow\rightarrow NO_3^- + H^+ \quad [k_{10} = 0.7\ s^{-1}] \qquad (10)$$

$$HOONO \rightleftarrows [^{\bullet}OH + {}^{\bullet}NO_2]_{cage} \qquad (11)$$

$$[^{\bullet}OH + {}^{\bullet}NO_2]_{cage} \rightarrow NO_3^- + H^+ \qquad (12)$$

$$[^{\bullet}OH + {}^{\bullet}NO_2]_{cage} \rightleftarrows {}^{\bullet}OH + {}^{\bullet}NO_2 \qquad (13)$$

The formation of nitrate/nitric acid in reaction 12 cannot account for nitrophenol formation in the presence of HOONO. Actually, no nitration of 1.0×10^{-3} M P has been observed in the dark in the presence of 1.0×10^{-2} M HNO_3 (pH 2.0 (*14*)). In the case of Figure 1 in this paper, the maximum achievable $[HNO_3]$ is 1.0×10^{-3} M at pH 3.0. This observation also indicates that nitration in the presence of peroxynitrous acid occurs at a far higher rate and under much milder conditions than nitration by the stable isomer, nitric acid.

Nitration of P and P derivatives has been studied in the presence of peroxynitrite (*36*, *37*). The cited authors have proposed electrophilic nitration pathways, involving however different species. In the case of peroxynitrous acid, nitration processes can take place upon generation of nitrogen dioxide (reactions 11 and 13) or in the presence of other nitrating agents (e.g. NO^+ and NO_2^+ that might both form in acidic solution upon protonation of HOONO (*37*)).

From the point of view of the environmental significance it is important to assess the pH trend of nitrophenol formation in the presence of $HNO_2 + H_2O_2$. The interpretation of these results requires however the knowledge of the pH effect on the kinetics of reaction 6. Halfpenny and Robinson (*30*) have found that the rate is proportional to $[HNO_2] \times [H_2O_2] \times [H^+]$. The effect of H^+ has been thought to be due to the protonation of HNO_2, but the study has been performed in a limited pH interval (4−5), due to the need of limiting the reaction rate at a measurable level. To overcome this problem, we carried out fast kinetic experiments with a stopped-flow spectrophotometer.

Figure 2 shows the initial disappearance rate of nitrous acid in the presence of hydrogen peroxide as a function of $C_{H2O2} \times C_{NaNO2}$, where $C_{NaNO2} = [HNO_2] + [NO_2^-]$, at pH 2.0 (see also Table 1, entries #2−14; the table also reports $\alpha_{HNO2} = [HNO_2]/\{[HNO_2]+[NO_2^-]\}$, the p$K_a$ of nitrous acid being about 3.2 (*38*)). The dependence of $-d[HNO_2]/dt$ on $C_{H2O2} \times C_{NaNO2}$ is linear, and the disappearance rate of HNO_2 alone, without H_2O_2, is negligible at the adopted time scales (10 s reaction time, see also Table 1, entry #1). Figure 3 shows the initial disappearance rate of nitrous acid ($C_{NaNO2} = 5 \times 10^{-3}$ M) upon reaction with 0.010 M hydrogen peroxide, as a function of pH (see also Table 1, entries #15−22). Among the species that can influence the pH trend, $H_3O_2^+$ has pK_a = 1.5−2.0 (*39*) and protonated nitrous acid pK_a = −6.5 (*40*, *41*). The form in which protonated nitrous acid exists in solution ($H_2NO_2^+$ or NO^+) is still under debate (*41*). As shown in Figure 3, the pH trend is consistent with a reaction between either $H_3O_2^+$ and HNO_2 or H_2O_2 and protonated nitrous acid ($HNO_2 + H^+$), while a reaction between HNO_2 and H_2O_2 or between $H_3O_2^+$ and protonated nitrous acid can be ruled out. Our data allow the evaluation of the pK_a of $H_3O_2^+$ (1.47 ± 0.02).

From the results reported in Figures 2 and 3 and in Table 1, it is possible to derive the kinetic law for the disappearance rate of nitrous acid in the presence of hydrogen peroxide

$$-\frac{d[HNO_2]}{dt} = k^* \cdot \frac{[H^+]^2}{(K_{a,H3O2^+} + [H^+])(K_{a,HNO2} + [H^+])} \cdot C_{H2O2} \cdot C_{NaNO2} \qquad (14)$$

where $K_{a,H3O2+} = 3.4 \times 10^{-2}$ (p$K_{a,H3O2+} = 1.47$), $K_{a,HNO2} = 6 \times 10^{-4}$ (p$K_{a,HNO2} = 3.2$), and $k^* = 179.6 \pm 1.4\ M^{-1}\ s^{-1}$. If the reaction involves $H_3O_2^+$ and HNO_2, k^* would be their second-order rate constant. If the reaction occurs between H_2O_2 and protonated nitrous acid, $k^* = k' \times K_{a,H3O2+}/K_{a,HNO2+H+}$ (if $[H^+] \ll 10^{6.5}$), where $k' = (1.68 \pm 0.01) \times 10^{10}\ M^{-1}\ s^{-1}$ would be the rate constant for the bimolecular reaction between H_2O_2 and protonated nitrous acid. Such a reaction thus needs to be diffusion controlled to account for the observed rates (the concentration of protonated nitrous acid in a 5×10^{-3} M solution of HNO_2 at pH 2.0 is only 1.6×10^{-11} M). For this reason peroxynitrous acid seems more likely to derive from $H_3O_2^+$ and HNO_2.

The pH trend of the initial formation rates of 2NP and 4NP is reported in Figure 4 (see also Table 2, entries #1−6). The fitting of the experimental data with rate ∝ $-d[HNO_2]/dt$ is rather poor (see the dotted lines in Figure 4). Actually, the initial formation rates of both 2NP and 4NP are proportional to $[H^+]$ (Figure 4, solid lines), as would be expected in the case of an electrophilic nitration pathway.

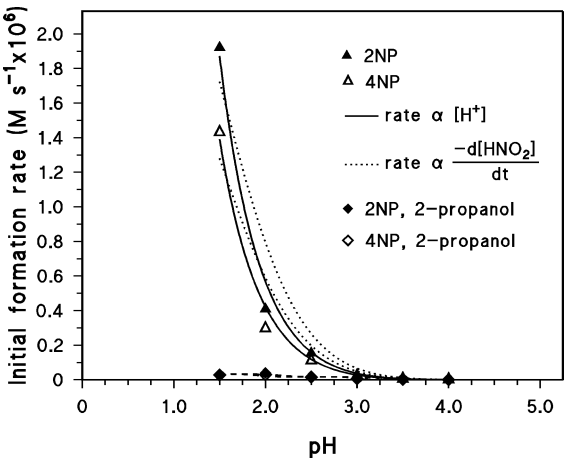

FIGURE 4. Initial formation rates of 2NP and 4NP in the presence of 2.0×10^{-4} M P, 1.0×10^{-3} M $NaNO_2$, and 1.0×10^{-3} M H_2O_2, in the dark, as a function of pH (adjusted by addition of $HClO_4$). The initial formation rates of 2NP and 4NP in the same system, but upon addition of 0.10 M 2-propanol, are also reported.

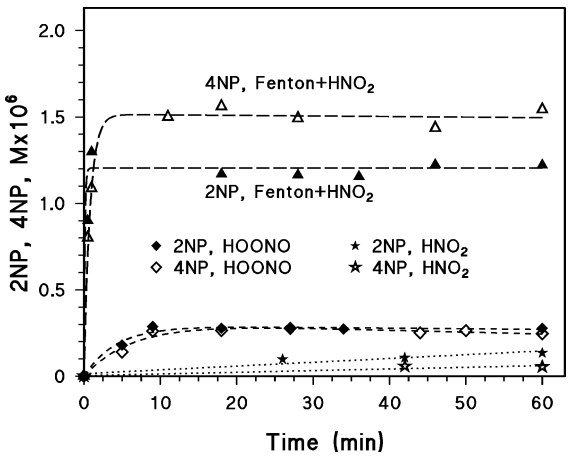

FIGURE 5. Time evolution of 2NP and 4NP in the presence of 2.0×10^{-4} M P and 1.0×10^{-3} M Fe(II) + H_2O_2 + $NaNO_2$, H_2O_2 + $NaNO_2$, $NaNO_2$ alone, in the dark. pH 5.0 by addition of $HClO_4$.

The single likely alternative to electrophilic nitration is linked with the formation of $^{\bullet}NO_2$ in the equilibrium reaction 13, although it is difficult to account for the pH effect shown in Figure 4 in the case of an $^{\bullet}NO_2$-initiated nitration. The latter process would however be enhanced by the addition of $^{\bullet}OH$ scavengers to the system, reacting with the hydroxyl radical and shifting the equilibrium reaction 13 toward the products, thus increasing the generation rate of nitrogen dioxide (*11*, *14*, *42*). The initial formation rates of 2NP and 4NP as a function of pH upon addition of 0.10 M 2-propanol, used as hydroxyl scavenger (*14*, *42*), are reported in Figure 4 (see also Table 2, entries #7−12). 2-Propanol strongly inhibits nitrophenol formation, which rules out $^{\bullet}NO_2$ as a possible nitrating agent in the system. A nitration process initiated by a species different from $^{\bullet}NO_2$ and forming from HOONO would be inhibited by 2-propanol because the shift of equilibrium reaction 13 toward the products would lead to a faster consumption of HOONO. As an alternative, 2-propanol might react with the nitrating agent (relevant reaction between 2-propanol and $^{\bullet}NO_2$ can be excluded (*14*, *20*)). The data are thus consistent with an electrophilic nitration pathway. Interestingly, phenol nitration by peroxynitrite has been proposed to be electrophilic, too (*36*, *37*).

The formation rate of nitrophenols in the presence of H_2O_2 and HNO_2 is very high at pH ≤ 3.0, but it is strongly pH-dependent and decreases as pH increases. The nitration rate by HOONO at pH 4.0 is however almost an order of magnitude higher than in the presence of HNO_2 alone (see Table 2, entries #6 and #13). The formation of peroxynitrous acid is thus a potential source of nitrophenols in acidic aerosols. Furthermore, the reaction between $H_3O_2^+$ and HNO_2 is not the only source of peroxynitrous acid in the environment, as this compound also forms in reactions 7−8. As a consequence, aromatic nitration by HOONO can be expected to occur also at pH values around neutrality, although at a reduced rate. Indeed, the condensed-phase nitration of aromatics is much more likely to occur in the presence of HOONO than of HNO_3.

Fe(II)/H_2O_2/NO_2^-. The Fenton reagent (Fe(II) + H_2O_2) is a long-known oxidant, which has found practical application in the decontamination of water and wastewater from organic contaminants (*43*). Its mechanism of action is traditionally thought to involve generation of $^{\bullet}OH$ radicals (reaction 15), although recent studies indicate that $^{\bullet}OH$ is probably not the only oxidant present in the system (*44*−*47*).

$$Fe(II) + H_2O_2 \rightarrow Fe(III) + {}^{\bullet}OH + OH^- \qquad (15)$$

Furthermore, the Fenton reaction is thought to play a relevant role as a source of oxidizing species in atmospheric acidic water droplets (*17*).

The rate constant of the reaction between Fe(II) and hydrogen peroxide has been found to be 63 M^{-1} s^{-1} at 25 °C (*47*). The generation rate of the hydroxyl radical (and/or other oxidants) is pH-dependent, and many authors have found an optimum pH value around 3 (*48*, *49*). At pH 5.0 the cited rate is about one-third than that at pH 3.0 (*49*).

If Fe(II), H_2O_2, and HNO_2 are present together in the system, there is competition between Fe(II) and HNO_2 for reaction with hydrogen peroxide. The rates of both reactions depend on pH, but the rate of the one involving HNO_2 decreases more sharply with increasing pH (see Figure 3 and eq 14). We chose pH 5.0 and used equimolar concentrations of Fe(II), H_2O_2, and NO_2^- + HNO_2 (all 1.0×10^{-3} M); in such a case it is possible to be confident that Fe(II) would react with H_2O_2 to form $^{\bullet}OH$ (and/or other oxidizing species), which would then oxidize NO_2^- and HNO_2 to nitrogen dioxide, excluding the peroxynitrous acid pathway. Figure 5 shows the time evolution of 2NP and 4NP forming from 2.0×10^{-4} M phenol, in the presence of Fe(II) + H_2O_2 + $NaNO_2$/HNO_2, of H_2O_2 + $NaNO_2$/HNO_2, and of $NaNO_2$/HNO_2 alone (see also Table 2, entries #14−16). Nitrophenol formation is faster in the presence of H_2O_2 + $NaNO_2$/HNO_2 than of $NaNO_2$/HNO_2 alone, due to the formation of peroxynitrous acid in the former case. In the case of the Fenton reaction (Fe(II) + H_2O_2 + $NaNO_2$/HNO_2) the initial formation rate of nitrophenols is by far the highest one, indicating the potentially relevant role that the Fenton oxidation of nitrite/nitrous acid to nitrogen dioxide has as a source of nitrophenols in atmospheric aerosols. Also the plateau concentration of 2NP and 4NP is higher in the case of the Fenton reaction when compared with the case of HOONO. Actually, the Fenton reaction leads to a quantitative production of oxidizing species (reaction 15), which can then react with either P or NO_2^-/HNO_2. The reaction with NO_2^- prevails at the adopted pH and concentration values (*50*) and yields nitrogen dioxide, which is in equilibrium with the dimer N_2O_4. The mixture $^{\bullet}NO_2$/N_2O_4 can either undergo hydrolysis or nitrate P. In the case of 2.0×10^{-4} M phenol the hydrolysis and nitration rates are comparable (*51*). The plateau concentration of nitrophenols is lower in the case of peroxynitrous acid because the main transformation pathway of HOONO is the isomerization to nitric acid (*34*), which does not lead to nitrophenols under the adopted conditions, while only a small fraction of HOONO is involved in the nitration reactions.

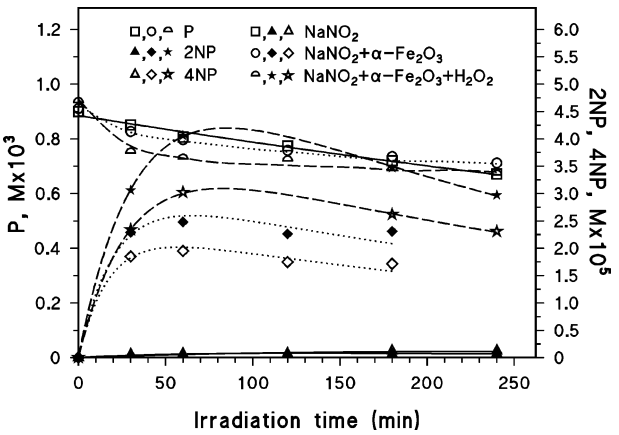

FIGURE 6. Time evolution of P, 2NP, and 4NP in the presence of P + $NaNO_2$, of P + $NaNO_2$ + α-Fe_2O_3, and of P + $NaNO_2$ + α-Fe_2O_3 + H_2O_2. Conditions: 1.0 × 10^{-3} M P, 1.0 × 10^{-3} M $NaNO_2$, 0.20 g/L α-Fe_2O_3, 1.0 × 10^{-2} M H_2O_2, pH 6.0, irradiation at 360 nm.

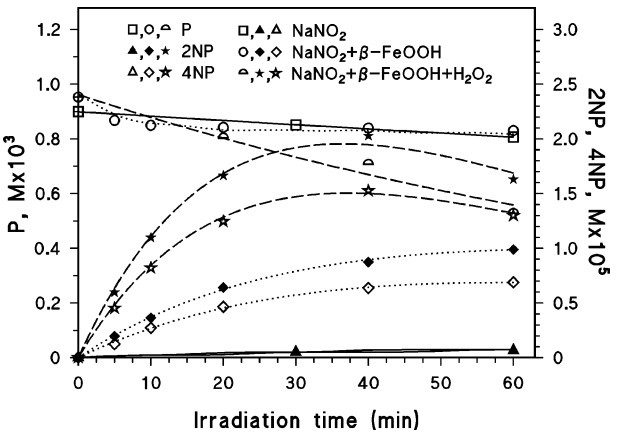

FIGURE 7. Time evolution of P, 2NP, and 4NP in the presence of P + $NaNO_2$, of P + $NaNO_2$ + β-FeOOH, and of P + $NaNO_2$ + β-FeOOH + H_2O_2. Conditions: 1.0 × 10^{-3} M P, 1.0 × 10^{-3} M $NaNO_2$, 0.20 g/L β-FeOOH, 1.0 × 10^{-2} M H_2O_2, pH 6.0, irradiation at 360 nm.

α-Fe_2O_3/NO_2^-/H_2O_2/UV and β-FeOOH/NO_2^-/H_2O_2/UV. The atmospheric occurrence of Fe(II) is linked with reduction or photolysis of Fe(III). The photolysis of Fe(III) in the presence of hydrogen peroxide constitutes the so-called photo-Fenton process (*43*). The homogeneous photo-Fenton process requires the presence of dissolved Fe(III), and only at pH ≤ 2.0 one can be confident that virtually all Fe(III) is dissolved (*52*). At higher pH the formation of Fe(III) hydroxide colloids can be relevant. However, it is not possible to study the nitration of P upon irradiation of Fe(III), H_2O_2, and HNO_2 at pH 2.0 or lower, due to the very fast thermal reaction between $H_3O_2^+$ and HNO_2 to yield peroxynitrous acid, HOONO, which induces phenol nitration. The problem of the formation of peroxynitrous acid can be overcome at pH ≥ 6.0, since negligible reaction occurs at room temperature between nitrite and hydrogen peroxide, and a suitable way of generating Fe(II) under such conditions is the photolysis of ferric (hydr)oxides (heterogeneous photo-Fenton process). α-Fe_2O_3 and β-FeOOH are semiconductor oxides, with indirect band gap absorption in the visible. α-Fe_2O_3 absorbs radiation at λ < 530 nm (*53*), β-FeOOH at λ < 575 nm (*26*). The irradiation of these oxides at λ > 430 nm produces electron−hole couples, which can then oxidize dissolved molecules. P nitration is strongly enhanced upon irradiation of nitrite and ferric oxides under such conditions (*20*).

Irradiation of α-Fe_2O_3 at λ < 375 nm causes excitation of a charge-transfer band, involving surface species (*54*):

$$Fe^{III}\text{-}OH + h\nu \rightarrow Fe(II) + {}^{\bullet}OH \qquad (16)$$

Reaction 16 causes photodissolution of α-Fe_2O_3, which occurs more rapidly in the presence of reducing species forming surface complexes, such as oxalate (*55*). A similar process would also take place in the case of β-FeOOH, which can be expected to have a higher surface density of Fe^{III}-OH groups than α-Fe_2O_3.

Figure 6 shows the time evolution of P, 2NP, and 4NP at pH 6.0 upon 360 nm irradiation of 1.0 × 10^{-3} M P in the presence of 1.0 × 10^{-3} M $NaNO_2$, 1.0 × 10^{-3} M $NaNO_2$ + 0.20 g/L α-Fe_2O_3, and 1.0 × 10^{-3} M $NaNO_2$ + 0.20 g/L α-Fe_2O_3 + 1.0 × 10^{-2} M H_2O_2. The initial degradation rate of P and the initial formation rates of 2NP and 4NP are also listed in Table 3, entries #1−3. A very marked increase in the initial formation rates of 2NP and 4NP can be observed in the presence of $NaNO_2$ + α-Fe_2O_3 with respect to $NaNO_2$ alone. The 360 nm irradiation induces both reaction 16 and the promotion of electrons from the valence to the conduction band (reaction 17). The oxidation of nitrite to nitrogen dioxide can take place either via reaction 2 or via reaction 18 (*20*):

$$\alpha\text{-}Fe_2O_3 + h\nu \rightarrow h^+ + e^- \qquad (17)$$

$$NO_2^- + h^+ \rightarrow {}^{\bullet}NO_2 \qquad (18)$$

In the presence of hydrogen peroxide, a further increase in the initial formation rates of 2NP and 4NP can be observed. This effect is most likely due to the Fenton reaction, involving photogenerated Fe(II) (*56*) and inducing additional oxidation of nitrite to nitrogen dioxide (reaction sequence: 16, 15, and 2). The effect of H_2O_2 cannot be accounted for by its photolysis to yield $^{\bullet}OH$, since the 360 nm irradiation of a mixture of H_2O_2 and $NaNO_2$ does not produce nitrophenols at a higher extent than the irradiation of $NaNO_2$ alone.

Figure 7 is analogous to Figure 6, with the difference that β-FeOOH was added instead of α-Fe_2O_3. The corresponding initial rates of P, 2NP, and 4NP are listed in Table 3, entries #1 and #4−5. The initial formation rates of 2NP and 4NP are higher in the presence of $NaNO_2$ + β-FeOOH when compared with $NaNO_2$ alone, due to the contribution of reactions 17−18 (*20*) and of reactions 16 and 2. The addition of H_2O_2 further increases the initial formation rates of 2NP and 4NP, due to the additional contribution of reactions 15 and 2.

Environmental Significance. The aqueous systems containing hydrogen peroxide and nitrite/nitrous acid can induce a relevant production of nitrophenols from phenol. A first pathway occurs in the presence of H_2O_2 and HNO_2 where HOONO forms a nitrating agent precursor. In the presence of Fe(II) and H_2O_2, the Fenton reaction can lead to the oxidation of both nitrite and nitrous acid to nitrogen dioxide, inducing phenol nitration. Fe(II) can be generated in atmospheric aerosols upon illumination of Fe(III) (hydr)-oxides (heterogeneous photo-Fenton reaction). The described processes have a potentially relevant role in the condensed-phase chemistry of the atmosphere. Furthermore, toxic nitroderivatives can form upon treatment of nitrite-containing water at acidic pH, in the presence of H_2O_2 or of the Fenton reagent (Fe(II) + H_2O_2).

Scheme 1 shows the various transformation processes for phenol in the different systems we studied, based on the reported results and in analogy with refs *14*, *19*, *20*, *24*, and *51*. In each system particular reactive species (in brackets) are present, those having the major impact on phenol transformation being reported in bold: H_2O_2/HNO_2 (**electrophilic nitration species (e.g. NO_2^+ and NO^+)**, **$^{\bullet}OH$**, HNO_2, $^{\bullet}NO_2/N_2O_4$), Fe(II)/H_2O_2/HNO_2+NO_2^- (**$^{\bullet}NO_2/N_2O_4$**, **$^{\bullet}OH$**, HNO_2,

SCHEME 1. Phenol Transformation Pathways in the Systems under Study[a]

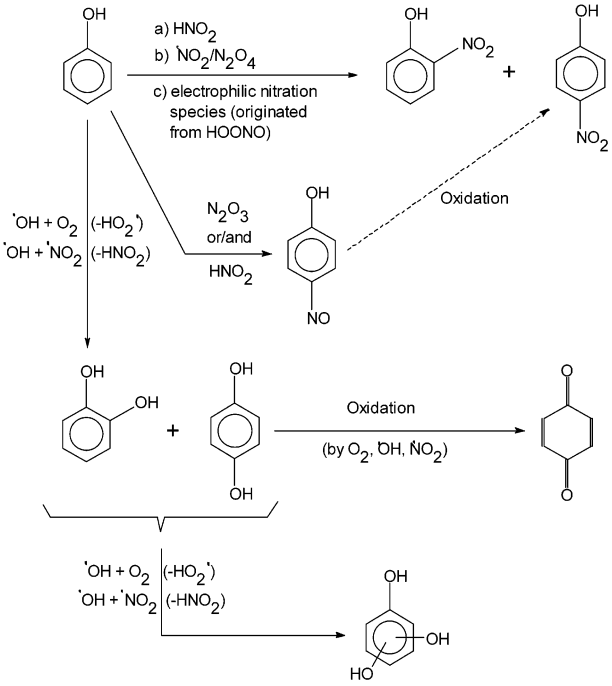

[a] The dashed arrows are relative to pathways that are negligible in all the systems we studied. As far as the formation of nitrophenols is concerned, the relative weight of the various pathways is discussed in the text (it varies according to the system under consideration).

electrophilic nitration species), α-Fe_2O_3/NO_2^-/H_2O_2/UV and β-FeOOH/NO_2^-/H_2O_2/UV (**$^{\bullet}NO_2/N_2O_4$**, **$^{\bullet}OH$**, N_2O_3).

Acknowledgments

Financial support of CNR − Agenzia 2000, Italian Interuniversity Consortium "Chemistry for the Environment" (INCA), PNRA − Progetto Antartide and Università di Torino − Ricerca Locale is kindly appreciated.

Literature Cited

(1) Finlayson-Pitts, B. J.; Pitts Jr., J. N. *Science* **1997**, *276*, 1045−1052.
(2) Atkinson, R.; Arey, J. *Environ. Health Persp.* **1994**, *102*, 117−126.
(3) Enya, T.; Suzuki, H.; Watanabe, T.; Hirayama, T.; Himasatsu, Y. *Environ. Sci. Technol.* **1997**, *31*, 2772−2776.
(4) Grosjean, D. *Environ. Sci. Technol.* **1985**, *19*, 968−974.
(5) Atkinson, R.; Aschmann, S. M.; Arey, J. *Environ. Sci. Technol.* **1992**, *28*, 1397−1403.
(6) Leuenberger, C.; Czuczwa, J.; Tremp, J.; Giger, W. *Chemosphere* **1988**, *17*, 511−515.
(7) Sasaki, J.; Aschmann, S. M.; Kwok, E. S. C.; Atkinson, R.; Arey, J. *Environ. Sci. Technol.* **1997**, *31*, 3173−3179.
(8) Pitts Jr., J. N.; Arey, J.; Zielinska, B.; Winer, A. M.; Atkinson, R. *Atmos. Environ.* **1985**, *19*, 1601−1608.
(9) Wang, H.; Hasegawa, K.; Kagaya, S. *Chemosphere* **1999**, *39*, 1923−1936.
(10) Sugiyama, H.; Watanabe, T.; Hirayama, J. *J. Health Sci.* **2001**, *47*, 28−35.
(11) Machado, F.; Boule, P. *J. Photochem. Photobiol. A: Chem.* **1995**, *86*, 73−80.
(12) Dzengel, J.; Theurich, J.; Bahnemann, D. W. *Environ. Sci. Technol.* **1999**, *33*, 294−300.
(13) Barletta, B.; Bolzacchini, E.; Meinardi, S.; Orlandi, M.; Rindone, B. *Environ. Sci. Technol.* **2000**, *34*, 2224−2230.
(14) Vione, D.; Maurino, V.; Minero, C.; Vincenti, M.; Pelizzetti, E. *Chemosphere* **2001**, *44*, 237−248.
(15) Vione, D.; Maurino, V.; Minero, C.; Pelizzetti, E. *Int. J. Environ. Anal. Chem.*, in press.
(16) Beitz, T.; Bechmann, W.; Mitzner, R. *Chemosphere* **1999**, *38*, 351−361.
(17) Arakaki, T.; Miyake, T.; Hirakawa, T.; Sakugawa, H. *Environ. Sci. Technol.* **1999**, *33*, 2561−2565.
(18) Fischer, M.; Warneck, P. *J. Phys. Chem.* **1996**, *100*, 18749−18756.
(19) Vione, D.; Maurino, V.; Minero, C.; Pelizzetti, E. *Chemosphere* **2001**, *45*, 893−902.
(20) Vione, D.; Maurino, V.; Minero, C.; Pelizzetti, E. *Environ. Sci. Technol.* **2002**, *36*, 669−676.
(21) Vione, D.; Maurino, V.; Minero, C.; Pelizzetti, E. *Chemosphere* **2001**, *45*, 903−910.
(22) Benkelberg, H.-J.; Warneck, P. *J. Phys. Chem.* **1995**, *99*, 5214−5221.
(23) Hoigné, J. In *Aquatic Chemical Kinetics*; Stumm, W., Ed.; Wiley: New York, 1990; pp 43−70.
(24) Vione, D.; Maurino, V.; Minero, C.; Pelizzetti, E. *Ann. Chim. (Rome)* **2003**, *93*, 477−488.
(25) Walling, C. *Acc. Chem. Res.* **1975**, *8*, 125−131.
(26) Leland, J. K.; Bard, A. J. *J. Phys. Chem.* **1987**, *91*, 5076−5083.
(27) Calvert, J. G.; Pitts, J. N. *Photochemistry*; Wiley: New York, 1966; pp 780−786.
(28) Vione, D.; Maurino, V.; Minero, C.; Pelizzetti, E. *Ann. Chim. (Rome)* **2002**, *92*, 919−929.
(29) Al-Obaidi, U.; Moodie, R. B. *J. Chem. Soc., Perkin Trans. 2* **1985**, 467−472.
(30) Halfpenny, E.; Robinson, P. L. *J. Chem. Soc.* **1952**, 928−938.
(31) Løgager, T.; Sehested, K. *J. Phys. Chem.* **1993**, *97*, 6664−6669.
(32) Halfpenny, E.; Robinson, P. L. *J. Chem. Soc.* **1952**, 939−946.
(33) Mark, G.; Korth, H.-G.; Schuchmann, H.-P.; von Sonntag, C. *J. Photochem. Photobiol. A: Chem.* **1996**, *101*, 89−103.
(34) Goldstein, S.; Meyerstein, D.; van Eldik, R.; Czapski, G. *J. Phys. Chem. A* **1999**, *103*, 6587−6590.
(35) Gerasimov, O. V.; Lymar, S. V. *Inorg. Chem.* **1999**, *38*, 4317−4321.
(36) Uppu, R. M.; Lemercier, J. N.; Squadrito, G. L.; Zhang, H. W.; Bolzan, R. M.; Pryor, W. A. *Arch. Biochem. Biophys.* **1998**, *358*, 1−16.
(37) Nonoyama, N.; Chiba, K.; Hisatome, K.; Suzuki, H.; Shintani, F. *Tetrahedron Lett.* **1999**, *40*, 6933−6937.
(38) Martell, A. E.; Smith, R. M. *Critical Stability Constants*; Plenum Press: New York, 1974.
(39) Drexler, C.; Elias, H.; Fecher, B.; Wannowius, K. J. *Ber. Bunsen-Ges. Phys. Chem.* **1992**, *96*, 481−485.
(40) Bayless, N. S.; Dingle, R.; Watts, D. W.; Wilkie, R. J. *Aust. J. Chem.* **1963**, *16*, 933−940.
(41) Bell, K. E.; Kelly, H. C. *Inorg. Chem.* **1996**, *35*, 7225−7228.
(42) Warneck, P.; Wurzinger, C. *J. Phys. Chem.* **1988**, *92*, 6278−6283.
(43) Legrini, O.; Oliveros, E.; Braun, A. M. *Chem. Rev.* **1993**, *93*, 671−698.
(44) Yamazaki, I.; Piette, L. H. *J. Am. Chem. Soc.* **1991**, *113*, 7588−7593.
(45) Sawyer, D. T.; Kang, C.; Llobet, A.; Redman, C. *J. Am. Chem. Soc.* **1993**, *115*, 5817−5818.
(46) Bossmann, S. H.; Oliveros, E.; Göb, S.; Siegwart, S.; Dahlen, E. P.; Payawan Jr., L.; Straub, M.; Wörner, M.; Braun, A. M. *J. Phys. Chem. A* **1998**, *102*, 5542−5550.
(47) Pignatello, J. J.; Liu, D.; Huston, P. *Environ. Sci. Technol.* **1999**, *33*, 1832−1839.
(48) Gallard, H.; De Laat, J.; Legube, B. *New J. Chem.* **1998**, 263−268.
(49) Sedlak, D. L.; Andren, A. W. *Environ. Sci. Technol.* **1991**, *25*, 777−782.
(50) Buxton, G. V.; Greenstock, C. L.; Helman, W. P.; Ross, A. B. *J. Phys. Chem. Ref. Data* **1988**, *17*, 1027−1284.
(51) Vione, D. Ph.D. Thesis, University of Torino, Italy, 2001.
(52) Faust, B. C.; Hoigné, J. *Atmos. Environ.* **1990**, *24A*, 79−89.
(53) Faust, B. C.; Hoffmann, M. R.; Bahnemann, D. W. *J. Phys. Chem.* **1989**, *93*, 6371−6381.
(54) Faust, B. C.; Hoffmann, M. R. *Environ. Sci. Technol.* **1986**, *20*, 943−948.
(55) Siffert, C.; Sulzberger, B. *Langmuir* **1991**, *7*, 1627−1634.
(56) Mazellier, P.; Sulzberger, B. *Environ. Sci. Technol.* **2001**, *35*, 3314−3320.

Received for review February 10, 2003. Revised manuscript received July 4, 2003. Accepted July 10, 2003.

ES0300259